





An Infant Mouse Model of Influenza Virus Transmission Demonstrates the Role of Virus-Specific Shedding, Humoral Immunity, and Sialidase Expression by Colonizing *Streptococcus pneumoniae*

 Mila Brum Ortigoza,^a Simone B. Blaser,^b M. Ammar Zafar,^{c*} Alexandria J. Hammond,^c  Jeffrey N. Weiser^c

^aDepartment of Medicine, Division of Infectious Diseases, New York University School of Medicine, New York, New York, USA

^bNew York University School of Medicine, New York, New York, USA

^cDepartment of Microbiology, New York University School of Medicine, New York, New York, USA

ABSTRACT The pandemic potential of influenza A viruses (IAV) depends on the infectivity of the host, transmissibility of the virus, and susceptibility of the recipient. While virus traits supporting IAV transmission have been studied in detail using ferret and guinea pig models, there is limited understanding of host traits determining transmissibility and susceptibility because current animal models of transmission are not sufficiently tractable. Although mice remain the primary model to study IAV immunity and pathogenesis, the efficiency of IAV transmission in adult mice has been inconsistent. Here we describe an infant mouse model that supports efficient transmission of IAV. We demonstrate that transmission in this model requires young age, close contact, shedding of virus particles from the upper respiratory tract (URT) of infected pups, the use of a transmissible virus strain, and a susceptible recipient. We characterize shedding as a marker of infectiousness that predicts the efficiency of transmission among different influenza virus strains. We also demonstrate that transmissibility and susceptibility to IAV can be inhibited by humoral immunity via maternal-infant transfer of IAV-specific immunoglobulins and modifications to the URT milieu, via sialidase activity of colonizing *Streptococcus pneumoniae*. Due to its simplicity and efficiency, this model can be used to dissect the host's contribution to IAV transmission and explore new methods to limit contagion.

IMPORTANCE This study provides insight into the role of the virus strain, age, immunity, and URT flora on IAV shedding and transmission efficiency. Using the infant mouse model, we found that (i) differences in viral shedding of various IAV strains are dependent on specific hemagglutinin (HA) and/or neuraminidase (NA) proteins, (ii) host age plays a key role in the efficiency of IAV transmission, (iii) levels of IAV-specific immunoglobulins are necessary to limit infectiousness, transmission, and susceptibility to IAV, and (iv) expression of sialidases by colonizing *S. pneumoniae* antagonizes transmission by limiting the acquisition of IAV in recipient hosts. Our findings highlight the need for strategies that limit IAV shedding and the importance of understanding the function of the URT bacterial composition in IAV transmission. This work reinforces the significance of a tractable animal model to study both viral and host traits affecting IAV contagion and its potential for optimizing vaccines and therapeutics that target disease spread.

KEYWORDS animal models, influenza, transmission

Received 26 October 2018 **Accepted** 7 November 2018 **Published** 18 December 2018

Citation Ortigoza MB, Blaser SB, Zafar MA, Hammond AJ, Weiser JN. 2018. An infant mouse model of influenza virus transmission demonstrates the role of virus-specific shedding, humoral immunity, and sialidase expression by colonizing *Streptococcus pneumoniae*. mBio 9:e02359-18. <https://doi.org/10.1128/mBio.02359-18>.

Editor Keith P. Klugman, Emory University

Copyright © 2018 Ortigoza et al. This is an open-access article distributed under the terms of the [Creative Commons Attribution 4.0 International license](https://creativecommons.org/licenses/by/4.0/).

Address correspondence to Jeffrey N. Weiser, jeffrey.weiser@nyulangone.org.

* Present address: M. Ammar Zafar, Department of Microbiology and Immunology, Wake Forest School of Medicine, Winston-Salem, North Carolina, USA.

This article is a direct contribution from a Fellow of the American Academy of Microbiology. Solicited external reviewers: Florian Krammer, Icahn School of Medicine at Mount Sinai; Jonathan McCullers, The University of Tennessee Health Science Center.

Influenza virus infections continue to cause 140,000 to 700,000 hospitalizations and 12,000 to 56,000 deaths in the United States annually (1). For the 2017 to 2018 season alone, more than 900,000 people were hospitalized and 80,000 people died from influenza (2). Despite the availability of vaccines that have been efficacious at preventing hospitalizations, morbidity, and mortality, evidence that the inactivated influenza virus (IIV) vaccine blocks virus acquisition, shedding, or transmission has been limited in animal models (3–7). In addition, the low vaccination coverage (in the population) and low vaccine effectiveness (due to viral antigenic drift) likely contribute to the limited effects of the IIV vaccine (8, 9). Likewise, available therapeutics, primarily neuraminidase inhibitors (NIs), have been shown to be effective at reducing the duration of illness if treatment is initiated within 24 h of symptom onset (10–13). However, NI treatment of index cases alone shows limited effectiveness at reducing viral shedding or transmission, possibly due to its short therapeutic window (10, 11, 14, 15). These limitations of our current options to prevent disease spread highlight a critical aspect of the influenza A virus (IAV) ecology that needs further study: contagion.

While IAV transmission has been studied in human, ferret, and guinea pig models, there is a general lack of understanding about the host's influence on viral transmission, because none of these models are easily manipulated. Hence, scientific progress to date has emphasized viral genetics, viral tropism, and environmental impacts on transmission (16–19). While these factors contribute to knowledge about IAV contagion, host characteristics that could affect transmissibility, including the highly variable composition of the upper respiratory tract (URT) flora, remain largely unexplored.

This knowledge gap could be addressed with the use of mice, whose practical features (small, inexpensive, and inbred), expansive reagent repertoire, and availability of genetically modified hosts allow for studies of extraordinary intricacy providing a significant research advantage. Since the 1930s, the mouse model has been essential in understanding IAV immunity and pathogenesis, and early studies described its usefulness in evaluating IAV transmission (20, 21). However, the use of mice for studying IAV transmission has been largely disregarded due to marked differences among studies and low transmission rates (22–24). Nevertheless, recent reports have revived the potential of the murine species as an IAV transmission model (23–28). Therefore, in this study, we sought to reevaluate the mouse as a tool to study the biology of IAV contagion, particularly the contribution of host factors.

RESULTS

Infant mice support efficient influenza virus transmission. Given the remarkable capacity of infant mice to support IAV transmission among littermates (25), we sought to validate and optimize the infant mouse as a potential new model to study IAV transmission. Restricted URT infection of infant C57BL/6J pups in a litter (index) was performed with a low-volume intranasal (i.n.) inoculum (3 μ l) using IAV strain A/X-31 (H3N2) (24, 29). Intralitter transmission was assessed in littermates (contact/recipient) by measuring virus from retrograde tracheal lavages at 4 to 5 days postinfection (p.i.) (Fig. 1A). A/X-31 virus was selected to model transmission because of its intermediate virulence in mice (30) and ability to replicate in the URT to high titers with natural progression to the lungs, simulating key features of the infectious course in humans. Furthermore, the 50% mouse infectious dose (MID_{50}) in this model is 4 to 5 plaque-forming units (PFU), suggesting high susceptibility to A/X-31 infection. Transmission efficiency was observed to be 100% when index and contact pups were housed together at the time of IAV inoculation (Fig. 1B). Transmission declined the longer the index and recipient pups were housed apart prior to being in direct contact and was completely eliminated when mice were housed together after 72 h of separation (Fig. 1C; see Fig. S1 in the supplemental material). This observation suggested that in this model, transmission from index to recipient is most effective within the first 72-h period of contact.

To determine the window of viral acquisition in recipient mice, an 8-day IAV transmission experiment was performed (Fig. 1D). The observed growth of IAV in the

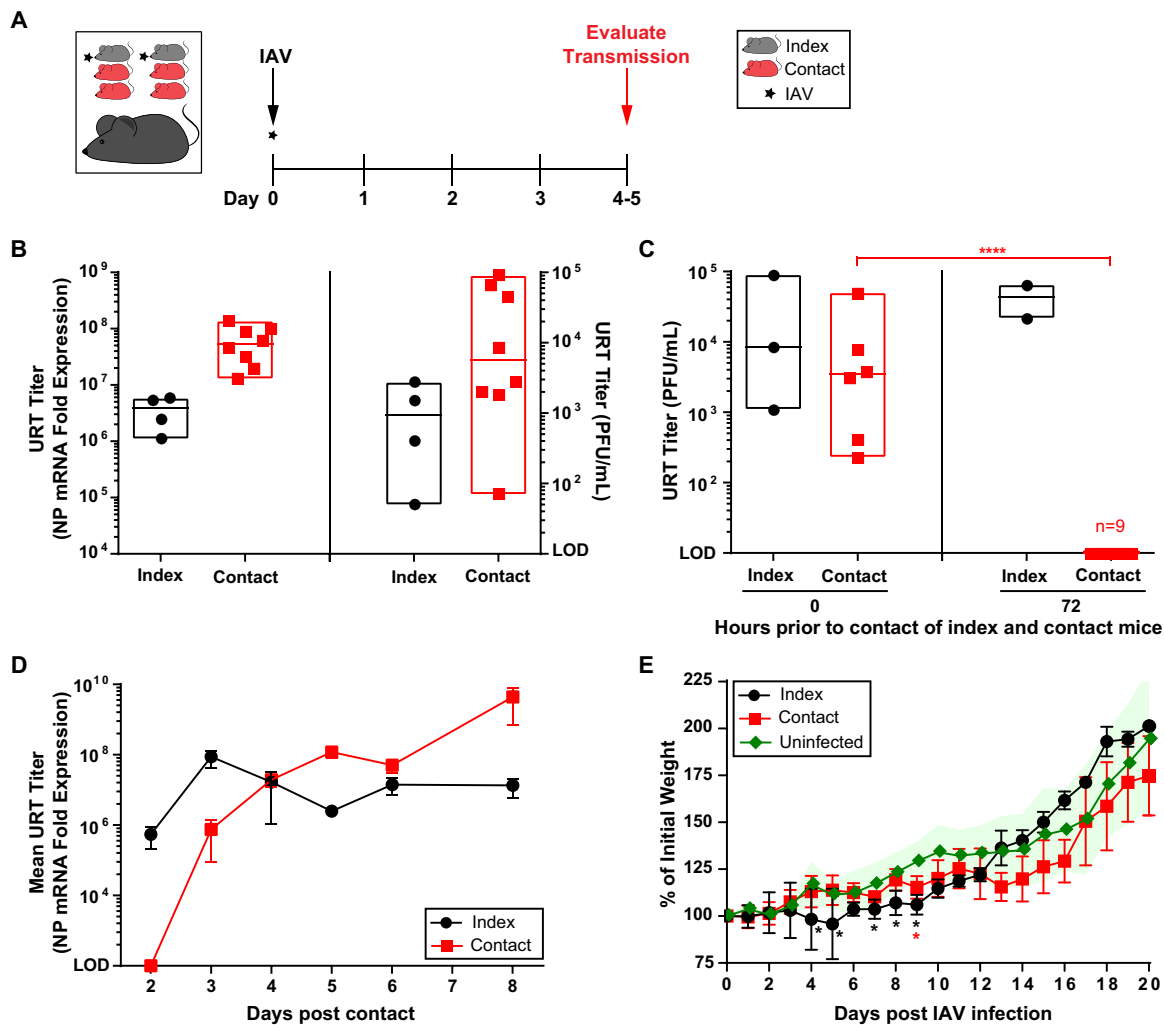


FIG 1 Transmission of IAV in infant mice. (A) Schematic and timeline of experimental design. Index and contact pups were arbitrarily assigned, maintained in the same cage, and cared for by the same mother. At day 0 (4 to 7 days of age), pups were infected i.n. with 250 PFU of A/X-31 (index) and cohoused with uninfected littermates (contact) for 4 to 5 days prior to being evaluated for transmission. (B) Transmission of IAV to contact pups was evaluated via qRT-PCR (left panel) or plaque assay (right panel) from retrograde URT lavages after sacrifice. URT titers are represented by a box plot extending from the minimum to maximum values for each data set. Each symbol represents the titer measured from a single pup, with median values indicated by a line within the box. Index and contact pups are shown by black and red symbols, respectively. (C) The window of transmission was evaluated by separating index and contact pups for a defined period prior to contact. Uninfected contact pups were housed apart (in a separate cage) for 0 and 72 h prior to cohousing with infected index pups for 5 days. Transmission to contact pups was evaluated via plaque assay from retrograde URT lavages. URT titers are represented by a box plot as described above. **** indicates statistical significance between Index and Contact groups at 72 hours. (D) Time course of A/X-31 transmission. Pups in a litter were subjected to an A/X-31 transmission experiment (described above), and transmission to contact pups was evaluated via qRT-PCR from retrograde URT lavages at indicated day post-contact. Mean URT titers \pm standard error of the mean (SEM) are represented. (E) Morbidity of A/X-31 infection in index and contact pups over the course of 20 days. Pups in a litter were subjected to an A/X-31 transmission experiment (described above), and the weight of each pup was measured daily. The percentage of initial weight \pm standard deviation (SD) is represented (uninfected group, $n = 9$; index group, $n = 3$ to 4; contact group, $n = 4$ to 5). Differences among group means were analyzed using the Student's t test. All panels represent at least two independent experiments. *, $P < 0.05$; ****, $P < 0.0001$. IAV, influenza A virus; URT, upper respiratory tract; NP, nucleoprotein; PFU, plaque-forming unit, LOD, limit of detection.

URT of recipient pups suggested that *de novo* virus acquisition occurred between 2 and 3 days after contact with the index. Hence, the infectious window for the index pups corresponded with the timing of IAV acquisition in contact pups.

Given that pups gain weight as they grow, morbidity in this model was assessed by observing a decrease in weight gain during the infectious period. Mild morbidity of pups was observed in both the index and contact groups, with complete recovery from IAV infection by 10 days p.i. (Fig. 1E).

Direct contact between pups is required for influenza virus transmission. Because infant mice need their mother for survival during the first 21 days of life, they

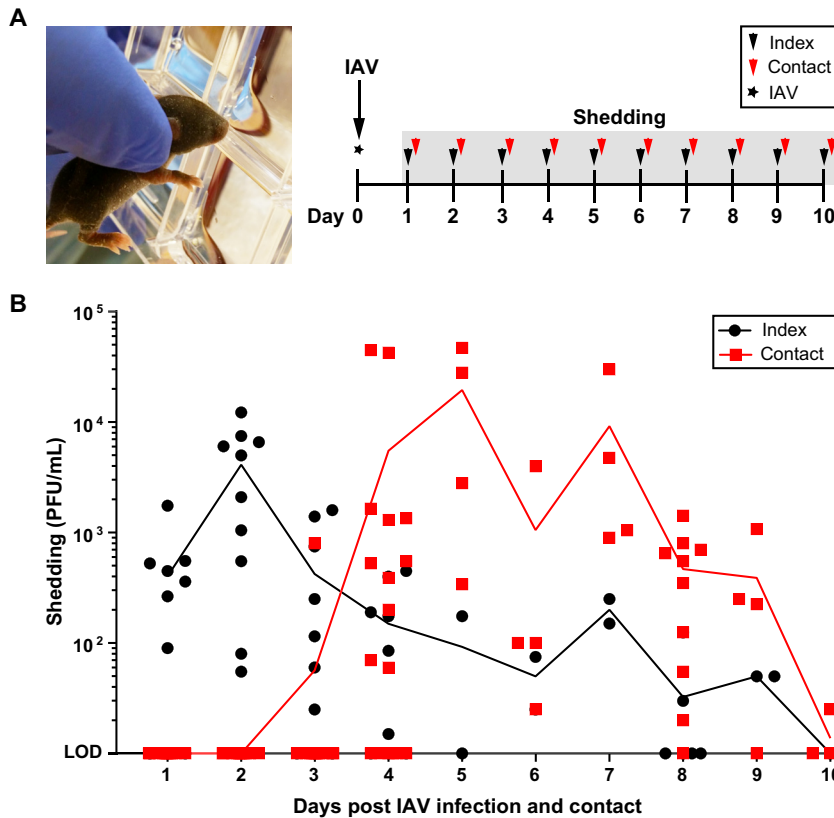


FIG 2 Shedding of IAV. (A) Image of infant mouse shedding procedure and schematic timeline of experimental design. At day 0 (4 to 7 days of age), pups were infected i.n. with 250 PFU of A/X-31 (index) and cohoused with uninfected littermates (contact) for 10 days. Shedding of IAV was collected by dipping the nares of each mouse in viral medium daily. (B) Shedding samples from each day were evaluated individually via plaque assay. Each symbol represents the shedding titer measured from a single mouse on the specified day. Index and contact pups are shown by black and red symbols, respectively. Mean values are connected by a line. IAV, influenza A virus; PFU, plaque-forming unit; LOD, limit of detection.

cannot be separately housed; therefore, this model cannot differentiate between the airborne versus droplet routes of transmission. To distinguish between direct and indirect contact routes of transmission, the mother and housing contents were evaluated as potential fomites. This was done by daily switching the mothers or the cages with bedding between infected and uninfected litters, respectively (see Fig. S2A and B in the supplemental material). Inefficient or no transmission was observed, suggesting that direct (close) contact between pups is the main mode of transmission. Occasionally during a transmission experiment, the mother in the cage became infected with IAV from close contact with her infected pups (Fig. S2C). Although the acquisition of IAV in the mother was a rare event, we did not observe a decline in transmission in contact pups when the mother did not become infected, despite the mother being capable of transmitting IAV to her pups if she were to be inoculated with IAV as the index case (Fig. S2D).

Role of shedding of influenza virus from the upper respiratory tract. To determine the correlates of transmission, an assay was developed to quantify infectious virus expelled from the nasal secretions of pups. This assay allowed us to follow the journey of particle exit from index pups to acquisition by contact pups over the course of the transmission period. Index pups in a litter were infected with A/X-31 and cohoused with uninfected littermates for 10 days. The nares of each mouse were gently dipped in viral medium daily, and virus titers were assessed for each sample (Fig. 2A). We observed that index pups, like in humans (31), began shedding virus from day 1 p.i.,

TABLE 1 Transmissibility of influenza viruses in infant mice

Virus	Index mice ^a			Contact mice ^b		Transmission (%) ^f
	No. infected ^c	URT titer ^d	Shedding titer ^e	No. infected ^c	URT titer ^d	
A/H3N2						
A/X-31 ^g	8/8	3.04 ± 1.32	2.20 ± 1.02	15/15	4.10 ± 1.05	100
A/Hong Kong/1/1968	4/4	4.85 ± 0.40	2.62 ± 0.67	8/8	5.64 ± 0.35	100
A/X-47 ^h	3/3	3.99 ± 0.25	2.13 ± 0.74	2/9	2.58 ± 2.31	22.2
A/H1N1						
A/Puerto Rico/8/1934	4/4	2.85 ± 0.56	NA ⁱ	2/13	2.51 ± 0.44	15.4
A/WSN/1933	6/6	4.18 ± 0.63	1.43 ± 0.64	1/10	NA	10
A/Brisbane/59/2007	5/5	2.50 ± 1.74	1.63 ± 0.75	1/12	NA	8.3
A/California/4/2009	5/5	3.77 ± 0.32	1.26 ± 0.42	0/12	NA	0
B						
B/Lee/1940	5/5	4.44 ± 0.93	2.58 ± 1.31	12/15	3.62 ± 1.67	80

^aIndex pups were infected i.n. with 250 PFU of virus.

^bUninfected contact pups were housed together with infected index pups at the time of inoculation for the duration of the experiment (4 to 8 days).

^cSum of index or contact pups assayed in at least 2 independent experiments.

^dURT titers, expressed as the mean log₁₀ PFU/ml ± SD, were assessed via plaque assay at time of sacrifice from retrograde tracheal lavages for each pup.

^eShedding titers, expressed as the mean log₁₀ PFU/ml ± SD, were assessed via plaque assay from daily shedding samples collected for each pup.

^fPercentage of contact pups containing detectable virus in the URT. A/H3N2 viruses were assayed after 4 days. A/PR/8, A/WSN, and B/Lee viruses were assayed after 4 and 8 days. A/Brisbane and A/California were assayed after 8 days.

^gHA/NA from A/Aichi/2/1968 (H3N2) plus genes from A/Puerto Rico/8/1934 (H1N1).

^hHA/NA from A/Victoria/3/1975 (H3N2) + genes from A/Puerto Rico/8/1934 (H1N1).

ⁱNA, data not applicable for any value representing fewer than 2 pups.

whereas recipient pups, who acquired IAV infection between days 2 and 3 (Fig. 1D), began shedding virus from day 4 post-contact (Fig. 2B). This pattern of virus transit suggested that the timing of peak shedding from the index (days 1 to 3) corresponded with the timing of transmission to recipient pups (days 2 to 4) (see Fig. S3 in the supplemental material) further confirming that a key determinant of IAV transmission in this model is shedding of virus from the secretions of index pups. Notably, detectable shedding in the contacts lagged transmission (higher transmission rate compared to number of contacts shedding virus), because of the period of viral replication required prior to the detection of shed virus (Fig. S3).

Transmission efficiency of influenza viruses in mice is virus and age dependent.

Virus strain has been shown to be important in the efficiency of transmission in adult mice (20, 23, 26, 32). We thus tested the capacity of infant mice to support transmission of other IAV subtypes and an influenza B virus (IBV) (Table 1). Transmission among pups was greater for influenza A/H3N2 viruses and IBV, but lower for A/H1N1 viruses. Notably, A/X-31 was more efficiently transmitted than its parent A/PR/8/1934 virus, suggesting that the hemagglutinin (HA) and/or neuraminidase (NA) proteins are responsible for efficient shedding and transmission of IAV in infant mice.

Surprisingly, the mean viral URT titers in index pups did not correlate with IAV transmission ($r = 0.315$), indicating that virus replication in the URT alone was insufficient to mediate effective transmission (see Fig. S4A in the supplemental material). To determine the cause of the differences in transmission efficiencies observed among virus strains, the shedding of each virus was analyzed. We observed that virus shed from index pups correlated with IAV transmission ($r = 0.8663$), further supporting virus shedding as the main determinant of IAV transmission efficiency in infant mice (see Fig. S4A and B).

Given the effectiveness of the infant mouse in supporting transmission of IAV, we evaluated the disparities of transmission efficiency previously reported in adult mice (20–23, 26). Mice infected with A/X-31 at different ages were housed with uninfected age-matched contacts, and transmission efficiency was assessed at 5 days p.i. (Table 2). We observed that 100% transmission was sustained in mice up to 7 days of age. Weaned and active adult mice (>28 days of age) failed to sustain efficient transmission altogether. Furthermore, mouse age correlated with transmission rate among contact

TABLE 2 Viral transmissibility among different mice ages

Mouse group by age (days) ^c	Index mice ^a		Contact mice ^b		Transmission (%) ^f
	No. infected ^d	URT titer ^e	No. infected ^d	URT titer ^e	
Unweaned					
4	3/3	4.17 ± 0.77	4/4	4.66 ± 0.50	100
7	7/7	4.40 ± 1.23	11/11	3.94 ± 1.04	100
14	9/9	3.12 ± 0.95	11/17	3.41 ± 1.00	64.7
21	4/4	3.21 ± 0.78	6/9	2.82 ± 0.78	66.7
Weaned ^g					
28	3/3	3.80 ± 0.86	0/6	NA ^h	0
35	5/5	3.15 ± 0.52	0/8	NA	0
56	6/6	2.50 ± 0.71	1/9	NA	11.1

^aIndex mice were infected i.n. with 250 PFU of virus.

^bUninfected age-matched contact mice were housed together with infected index mice at the time of inoculation for the duration of the experiment (5 days).

^cAge of mice expressed in days after birth.

^dSum of index or contact mice assayed in at least 2 independent experiments.

^eURT titers, expressed as the mean log₁₀ PFU/ml ± SD, were assessed via plaque assay at time of sacrifice from retrograde tracheal lavages for each mice.

^fPercentage of contact mice containing detectable virus in URT after 5 days of contact.

^gMice weaned from breastfeeding and separated from the mother.

^hNA, data not applicable for any value representing less than 2 pups.

mice ($r = -0.8346$) (Fig. S4C), confirming that in the murine model, the requirement for young age is necessary to support efficient IAV transmission. Although the transmission experiments in this study were done with an IAV inoculum of 250 PFU, and increasing the inoculum size to 10³ to 10⁵ PFU correlated with increasing IAV titers in the URT tract of index mice ($r = 0.9264$), inoculum size was not associated with more efficient transmission among adult mice ($r = -0.2582$) (Fig. S4D).

Humoral immunity from prior influenza virus infection limits shedding and transmission. To further validate the relationship of viral shedding and transmission, we evaluated the role of IAV-specific immunity in this model. Because pups are infected at a young age and lack a fully functional adaptive immune response, it was necessary to provide IAV immunity via the mother (from prior IAV infection), who would then transfer immunoglobulins to her pups either prenatally via transplacental passage or postnatally via breastfeeding. Pups from immune mothers who were subjected to an intralitter IAV transmission experiment shed significantly less virus over the first 5 days of infection compared to pups from nonimmune mothers (Fig. 3A, left). Reduced shedding was associated with decreased transmission (20%) among immune litters ($P < 0.0001$) (Fig. 3A, below graph). To determine if the passage of anti-IAV immunoglobulins occurred prenatally or postnatally, mothers were switched shortly after delivery such that an immune mother raised pups from a nonimmune mother or vice versa. These cross-foster experiments demonstrated that maternal passage of immunoglobulins either prenatally or postnatally decreased IAV shedding among all pups, and that transmission to contact pups was more efficiently blocked when maternal antibodies were passed postnatally via breastfeeding ($P < 0.01$) (Fig. 3A, right). IAV-specific serum IgG was detected in immune mothers and pups born to or cared for by immune mothers, with the transfer of IgG via breastfeeding yielding higher titer of antibodies in these pups (Fig. 3B). IAV-specific serum IgA was detected in previously infected mothers but unlike IgG was not passed to their pups in significant amounts (Fig. S4).

Streptococcus pneumoniae colonization of the upper respiratory tract decreases influenza virus acquisition via bacterial sialidase activity. There is increasing evidence of the important role of the host's gut microbiome on IAV-specific immunity in the respiratory tract (33, 34). Yet, there is only one study evaluating the role of the URT microbiota in IAV infection (35) and no studies on its effect on transmission. This is surprising given that the nasopharynx, a nonsterile environment extensively

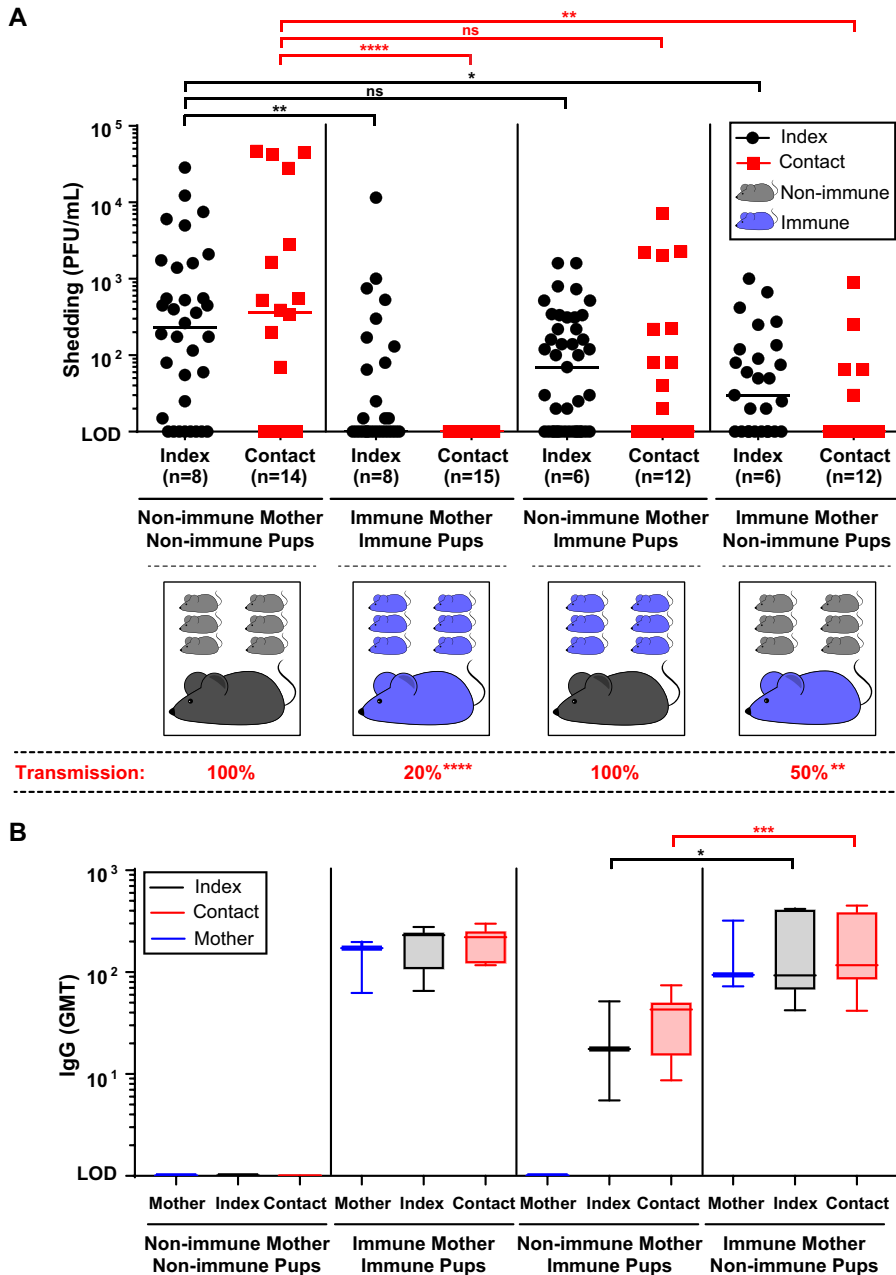


FIG 3 Maternal-infant transfer of IAV-specific immunity limits IAV shedding and transmission. (A) Adult females were infected i.n. with 250 PFU of A/X-31 and were left to recover from infection prior to breeding. Soon after birth, pups born from previously infected (immune) mothers or those born from nonimmune mothers were either left with their biological mother or exchanged with a foster mother of opposite immune status. Pups paired with their biological or foster mothers were left to acclimate until 4 to 5 days of life, prior to being subjected to an IAV transmission experiment. A schematic for each experimental condition is shown. Pups in a litter were infected i.n. with 250 PFU of A/X-31 (index) and cohoused with uninfected littermates (contact) for 5 days. Shedding of IAV was collected by gently dipping the nares of each mouse in viral medium daily. Shedding samples from each day were evaluated individually via plaque assay for each pup. The shedding titers shown represent pooled values for days 1 to 5 for index pups and days 4 to 5 for contact pups, representing days of maximum shedding for each group (as per Fig. 2). Each symbol represents the shedding titer measured from a single mouse for a specific day. Index and contact pups are shown by black and red symbols, respectively. Median values are indicated. At the end of 5 days, pups and mothers were sacrificed, and transmission to contact pups was evaluated via plaque assay from retrograde URT lavages. The percentage of transmission among contact pups is displayed below the graph. (B) Sera from mother and pups were obtained at the time of sacrifice. Samples from individual mice were evaluated for IAV-specific IgG by ELISA. IgG geometric mean titers (GMTs) are represented by a box plot extending from the 25th to 75th percentiles for each data set. Whiskers for each box encompass the minimum to maximum values. Median values are indicated by a line within the box. All panels represent

(Continued on next page)

colonized by a diverse bacterial flora, is the first location encountered by IAV. Since *Streptococcus pneumoniae* carriage is highest in children (36, 37), *S. pneumoniae* colonization often precedes IAV infection in childhood (38, 39). Given that infant mice support efficient *S. pneumoniae* colonization in the URT (25, 40), we investigated the impact of *S. pneumoniae* colonization on IAV transmission. All pups in a litter were colonized with *S. pneumoniae* prior to IAV infection of index pups to control for the efficient pup-to-pup transmission of *S. pneumoniae* in the setting of IAV infection (25). IAV shedding was collected daily for each pup prior to evaluation for IAV transmission in contact littermates at 4 days p.i. (Fig. 4A). We observed that the *S. pneumoniae*-colonized contact mice acquired IAV at a decreased rate (32%) compared to uncolonized mice (100%) ($P < 0.0001$) (see Fig. 4B, below graph), which corresponded to lower viral shedding among colonized contacts (Fig. 4B, left). Since index *S. pneumoniae* colonized and uncolonized mice infected with IAV (via inoculation) shed IAV at similar levels, this suggested an antagonistic effect of *S. pneumoniae* colonization on IAV transmission through decreased acquisition by contact mice.

Previous studies showed that sialidases expressed by colonizing *S. pneumoniae* deplete host sialic acid (SA) from the epithelial surface of the murine URT, allowing *S. pneumoniae* to utilize free SA for its nutritional requirements (41). Given that IAV requires SA for efficient attachment, we evaluated the role of *S. pneumoniae* sialidases on IAV acquisition. We generated a double mutant lacking two common *S. pneumoniae* sialidases: NanA and NanB (*nanA nanB* double-mutant), and tested its ability to alter IAV transmission in our system. These bacterial sialidases preferentially cleave 2,3-, 2,6-, and 2,8- or only 2,3-linked SA, respectively (42). We found that by colonizing mice with the *S. pneumoniae nanA nanB* double-mutant, we completely restored the efficiency of IAV transmission from 32% to 100% ($P < 0.0001$) (Fig. 4B, middle). We then tested the *nanA* and *nanB* single-sialidase mutants and found that the presence of NanA (via *nanB* mutant colonization) was sufficient to limit IAV acquisition by contacts to 25% ($P < 0.001$). Notably, there was no correlation between the colonization density of the bacterial mutants and their effect on shedding or transmission.

To determine the role of sialidases in general in IAV acquisition, infant index and contact mice were treated i.n. twice daily with *Vibrio cholerae* neuraminidase (VCNA), which cleaves both 2,3- and 2,6-linked sialic acids (43). We found that, like *S. pneumoniae* NanA, VCNA treatment was sufficient to decrease IAV acquisition (71.4%) and inhibit shedding by the contacts (Fig. 4B, right). Together, these observations suggest that sialidase activity from colonizing bacteria has the capacity to inhibit IAV acquisition in the URT, specifically via its cleavage of 2,3- and 2,6-linked SA.

DISCUSSION

The inability to study in detail the host's role in IAV transmission has been a major drawback of the ferret and guinea pig animal models and has limited our current understanding of IAV contagion (16–19). Herein we established an efficient and tractable infant mouse IAV transmission model with the goal of utilizing the extensive resources of mouse biology to explore the role that host factors, immune pathways, and the URT flora play in IAV transmission.

Our study corroborated previous findings that infant mice support efficient and consistent IAV transmission (20, 25) and document an age-dependent effect on the efficiency of transmission, highlighting inefficient transmission in adult mice. This suggests an inherent quality of younger mice (i.e., less mobility allowing closer contact, suckling, presence/absence of a host factor, microbiota composition, immunodeficient, or developmental status) that facilitates the shedding and transmissibility of IAV. In humans, young age correlates with increased IAV nasopharyngeal shedding (44) and

FIG 3 Legend (Continued)

at least two independent experiments. Differences in transmission were analyzed using Fisher's exact test. *, $P < 0.05$; **, $P < 0.01$; ***, $P < 0.001$; ****, $P < 0.0001$; ns, not significant; PFU, plaque-forming unit; LOD, limit of detection; GMT, geometric mean titer.

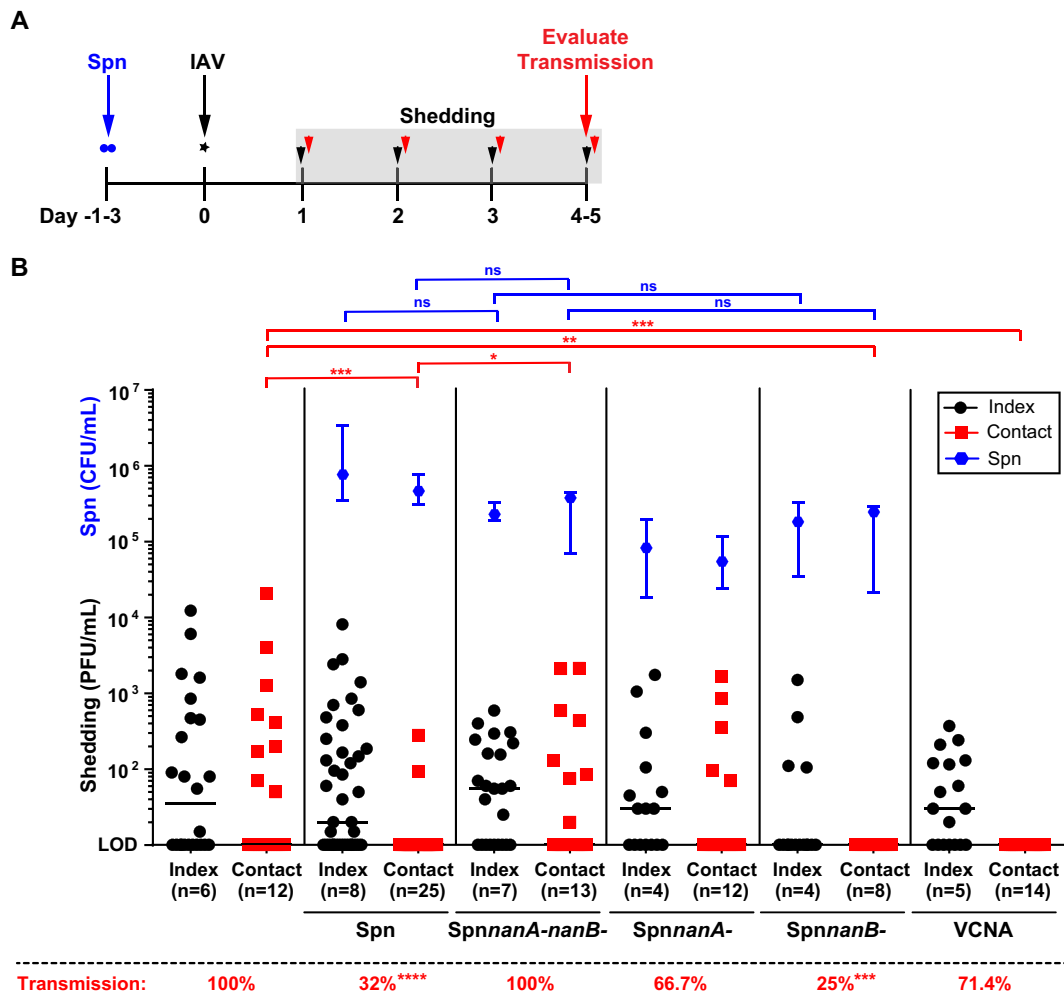


FIG 4 *Streptococcus pneumoniae* sialidases limit acquisition of IAV via transmission. (A) Schematic timeline of experimental design. At day -1 or -3 (3 to 4 days of age), all pups in a litter were colonized i.n. with either wild-type *S. pneumoniae* (Spn) or a mutant *S. pneumoniae* strain lacking NanA, NanB, or both or were treated i.n. with *Vibrio cholerae* neuraminidase (VCNA) twice daily. At day 0, pups were infected i.n. with 250 PFU of A/X-31 (index) and cohoused with uninfected littermates (contact) for 4 days. Shedding of IAV was collected by dipping the nares of each mouse in viral medium daily. Transmission to contact pups was evaluated at day 4. (B) Shedding samples from each day were evaluated individually via plaque assay for each pup. The shedding titers shown represent pooled values for days 1 to 4 for index pups and days 3 to 4 for contact pups. Each symbol represents the shedding titer measured from a single mouse for a specific day with median values indicated. Index and contact pups are shown by black and red symbols, respectively. At the end of 4 days, pups were sacrificed, and transmission to contacts was evaluated via plaque assay from retrograde URT lavages. The percentage of transmission among contact pups is displayed below the graph. Density of colonizing *S. pneumoniae* density was measured in URT lavage samples of each pup. Each blue symbol represents the median *S. pneumoniae* density \pm interquartile range for each group. Differences in transmission were analyzed using Fisher's exact test. *, $P < 0.05$; **, $P < 0.01$; ***, $P < 0.001$; ****, $P < 0.0001$; ns, not significant; Spn, *S. pneumoniae*; IAV, influenza A virus; PFU, plaque-forming unit; CFU, colony-forming unit; LOD, limit of detection.

longer duration of shedding (45), increasing the potential for transmission in this age group. Although it has been shown in the study of Edenborough (23) that 56-day-old adult mice support the transmission of A/X-31 and A/Udorn/307/72 (H3N2) viruses at 100% efficiency in BALB/c mice, we were unable to observe comparable efficiency in transmission using our A/X-31 virus in C57BL/6J mice older than 28 days. The work of Lowen (22) also failed to observe IAV transmission in adult BALB/c mice, further supporting an inconsistent transmission phenotype observed in adult mice, which has limited its utilization as an IAV transmission model. Notably, we are the first to demonstrate that infant mice support efficient IBV transmission, which contrasts with the inefficient IBV transmission previously reported in adult mice (32).

Although not evaluated in this study, the difference in mouse strains could also

affect the irregular success of IAV transmission in adult mice. One mouse strain, C57BL/6J, has been tested with infant mice and demonstrated 100% transmission efficiency in two independent studies (the present study and reference 25). In contrast, several mouse strains have been tested for IAV transmission among adult mice, with variable efficiencies among studies (0 to 100%) despite using similar virus strains. They include BALB/c (22, 23, 26, 28), C57BL/6J (present study), *Mx1*-competent C57BL/6J (24), Swiss Webster (20, 26, 46), New Colony Swiss (47), Manor Farms (MF-1) (32), DBA/2J (26), and Kunming (27). We learned from these studies that host traits (mouse age, strain, microbiota composition) all contribute to the infectivity and susceptibility of the murine species to IAV, and the host's contribution to transmission should be explored further using an efficient and tractable model of human disease.

Several studies have demonstrated that virus strain is an important determinant of IAV transmission in mice (20, 23, 32, 46, 48). Like more recent studies (23, 48), we highlighted the increased efficiency of transmission of A/H3N2 over A/H1N1 viruses. In addition, A/H2N2 viruses (not tested here) have also shown to have increased transmission efficiency in mice over A/H1N1 viruses (32, 46). Although we have not evaluated specific viral moieties that confer a transmissible phenotype, the viral HA has been demonstrated to play a role in transmission in mice (23). In addition, we postulate that the activity of some NA in combination with specific HA favors viral release from the nasal epithelium which allows viral shedding and transmission in mice. Thus, together, our data highlight that both host- and virus-specific features are important to consider to understand the requirements for IAV transmissibility.

We demonstrated that free virus particles present in secretions of mice, and not replicating virus in the URT, correlated with IAV transmission efficiency. A similar observation was also reported by Schulman (32), Edenborough (23), and Carrat (31) demonstrating that transmissibility was associated with greater shedding of virus in index mice, higher viral titers in the saliva of index mice, and shedding of virus from infected humans, respectively. These studies supported our conclusion that viruses that replicate in the URT without having the ability to exit the host (via shedding) cannot be transmitted efficiently. Additionally, studies by Milton (44) suggested that URT symptoms were associated with nasopharyngeal shedding in humans and that coughing was not necessary for the spread of infectious virus. This helps explain how mice, which lack the cough reflex, can still produce and shed infectious virions. This emphasizes an important future role of the infant mouse IAV transmission model as a tool to study viral shedding as a surrogate marker of IAV contagion.

Two host traits have been identified in this study that influence IAV transmission: IAV-specific immunoglobulin and the URT microbiota. The passive transfer of maternal immunity is via the placenta prenatally in an IgG-dependent manner (49, 50), or via breast milk postnatally mediated by several factors: immunoglobulins, leukocytes, and antimicrobial/anti-inflammatory factors (51–53). Our data recapitulates the value of maternal-infant transfer of IAV-specific IgG as a correlate of infant immunity, by demonstrating a significant inhibitory effect on viral shedding and transmission of infant mice after experimental (inoculation) and natural infection (via transmission). Our experiments also demonstrate that IAV-specific serum IgG is predominantly transferred via breastfeeding in mice, as previously reported (53, 54). The concept of maternal serum IgG passage via breast milk in mice has not often been recognized, even though it has been shown to occur (53, 55–57). IgG can be synthesized locally in the mammary gland, transferred across the mammary gland epithelium, and subsequently transported from the infant gut to the circulation via neonatal Fc receptors (FcRn) expressed in the proximal intestine (58–60). Although this mechanism of maternal IgG acquisition by infants has not yet been correlated in humans, the presence of FcRn in the human intestine has been confirmed (61, 62). Our study does not address the contribution of secretory IgA, which is known to be the most abundant immunoglobulin in breast milk. Yet, our data suggest that adequate amounts of IAV-specific IgG, which is known to wane within 8 weeks of birth in infants (63), may be necessary to maintain anti-IAV

immunity in the URT and limit IAV transmission in infants, given that at this young age, infants don't have a fully functional adaptive immune response.

In addition to humoral immunity, our study identified an inhibitory role for the common URT colonizer *S. pneumoniae* at the step of viral acquisition during transmission of IAV. This phenomenon has never been previously observed, although there has been some evidence suggesting that the preceding colonization of *S. pneumoniae* reduces IAV infection (25, 64). Notably, the study by McCullers (64) showed that preceding colonization with *S. pneumoniae* protected mice from mortality after IAV challenge, whereas the reverse process—prior infection with IAV with subsequent challenge with *S. pneumoniae*—yielded the opposite effect. This implied that the timing of pathogen encounter mattered, and the composition of the host microbiota may serve a “prophylactic-like” protective effect. Although no studies have evaluated the role of the respiratory microbiota on IAV transmission, we hypothesize that the differences between the transmissibility of different IAV strains and susceptibility of different populations (infants versus adults) to IAV may be due to a combined effect of the virus's ability to release from SA and exit the host via shedding, and the susceptibility to viral acquisition by contact hosts based on the composition of their URT microbiota. Our work provides proof of principle and highlights the amenability of the infant mouse model as a tool to understand the complex dynamics of virus and host, as well as their combined effect in IAV transmission.

Finally, we demonstrate the role of the *S. pneumoniae* sialidases NanA and NanB in antagonizing the acquisition and shedding of IAV by contact mice. We hypothesize that bacterium-driven desialylation of the host's URT glycoproteins for use as nutrient (41) may deplete SA residues necessary for IAV adhesion and infection, thus, limiting virus susceptibility and hence acquisition. Notably, the antagonistic effect of bacterial sialidases on IAV shedding of the index group is not statistically different from that of uncolonized controls. This is analogous to the clinical effects of NI, whereby oseltamivir treatment of index cases alone has not been shown to reduce viral shedding (10, 11). Only when treatment of both index and naive contacts was partaken (as in postexposure prophylaxis) was NI effective in preventing acquisition of infection among the contact group (12, 13). Because SA is the primary recognition moiety for many viral respiratory pathogens, the concept of utilizing bacterial sialidases as a broad antiviral agent is currently being explored in humans, although its effect on transmission has not yet been evaluated (65–72).

While the advantages of using murine models are evident, these can also be drawbacks. Humans are genetically diverse, live in complex environments, and have been exposed to a myriad of pathogens, all of which can affect transmissibility and susceptibility to IAV; therefore, findings generated in animal models of human disease should always be cautiously interpreted. Nevertheless, studying the complexities of IAV transmission biology in a tractable animal model such as infant mice, will allow intricate and sophisticated investigations, which will further our understanding of IAV contagion that may translate into better vaccines and therapeutics.

MATERIALS AND METHODS

Mice. C57BL/6J mice (Jackson Laboratories, ME) were maintained and bred in a conventional animal facility. Pups were housed with their mother for the duration of all experiments. Animal studies were conducted in accordance with the *Guide for the Care and Use of Laboratory Animals* (73) and approved by the Institutional Animal Care and Use Committee of NYU Langone Health (assurance no. A3317-01). All procedures were in compliance with *Biosafety in Microbiological and Biomedical Laboratories* (74).

Cells and viruses. Madin-Darby canine kidney (MDCK) cells were cultured in Dulbecco's modified Eagle's medium with 10% fetal bovine serum and 1% penicillin-streptomycin (Gibco).

A/X-31 (H3N2) virus (with HA/NA genes from A/Aichi/2/1968 and internal genes from A/Puerto Rico/8/1934) was a gift from Jan Erickson (University of Pennsylvania). The following reagents were obtained through BEI Resources (NIAID, NIH): A/X-47 (H3N2) (HA/NA genes from A/Victoria/3/1975 and internal genes from A/Puerto Rico/8/1934) (NR-3663), A/Hong Kong/1/1968-2 MA 21-2 (H3N2) (NR-28634), A/Puerto Rico/8/1934 (H1N1) V-301-011-000 (NR-3169), A/WSN/1933 (H1N1) (NR-2555), A/Brisbane/59/2007 (H1N1) (NR-12282), A/California/4/2009 (H1N1) (NR-13659), and B/Lee/1940 V-302-001-000 (NR-3178). IAV and IBV were propagated in 8- to 10-day-old embryonated chicken eggs (Charles River, CT) for 2 days at 37 and 33°C, respectively. Titers of all viruses were determined by standard plaque assay

in MDCK cells in the presence of TPCK (tolylsulfonyl phenylalanyl chloromethyl ketone)-treated trypsin (Thermo Scientific) (75). Purified virus for enzyme-linked immunosorbent assay (ELISA) was prepared by harvesting allantoic fluid from eggs containing virus followed by centrifugation ($3,000 \times g$, 30 min, 4°C) to remove debris. Viruses were pelleted through a 30% sucrose cushion (30% sucrose in NTE buffer [100 mM NaCl plus 10 mM Tris-HCl plus 1 mM EDTA], pH 7.4) by ultracentrifugation ($83,000 \times g$, 2 h), resuspended in phosphate-buffered saline (PBS), and stored at -80°C .

Virus infection, shedding, and transmission. Pups in a litter (4 to 7 days of age) were infected (index) with a $3 \mu\text{l}$ sterile PBS inoculum without general anesthesia (to avoid direct lung inoculation) by i.n. instillation of 250 PFU of IAV (unless otherwise specified) and returned to the litter at the time of inoculation for the duration of the experiment. Shedding of virus was collected by dipping the nares of each mouse into viral medium (PBS plus 0.3% bovine serum albumin [BSA]) daily, and samples were evaluated via plaque assay. Intralitter transmission was assessed in littermates (contact) at 4 to 5 days p.i. (days 10 to 14 of life). The pups and mother were euthanized by CO_2 asphyxiation followed by cardiac puncture, the URT was subjected to a retrograde lavage (flushing of $300 \mu\text{l}$ PBS from the trachea and collecting through the nares), and samples were used to quantify virus (via plaque assay or quantitative reverse transcription-PCR [qRT-PCR]) or *S. pneumoniae* density (described below). Ratios of index to contact pups ranged from 1:3 to 1:4.

Where indicated, pups were i.n. treated twice daily with $90 \mu\text{U}$ ($3 \mu\text{l}$ inoculum) of *Vibrio cholerae* neuraminidase (VCNA [Sigma-Aldrich]).

The MID_{50} was calculated by the method of Reed and Muench (76).

Induction of maternal IAV immunity. Adult female mice were infected i.n. with 250 PFU of A/X-31 in a $6 \mu\text{l}$ inoculum without anesthesia. Mice were left to recover from infection for 7 days prior to breeding. Litters of immune mothers were used in experiments.

Bacterial strain construction and culture. A streptomycin-resistant derivative of capsule type 4 isolate TIGR4 (P2406) was used in this study and cultured on tryptic soy agar (TSA)-streptomycin ($200 \mu\text{g}/\text{ml}$) plates (40). The *nanA* mutant strain (P2508) was constructed by transforming P2406 with genomic DNA from strain P2082 (77) (MasterPure DNA purification kit; Illumina) and selection on TSA-chloramphenicol ($2.5 \mu\text{g}/\text{ml}$) plates. The *nanB* mutant strain (P2511) was constructed by amplifying the Janus cassette (78) from genomic DNA of strain P2408 (79), with flanking upstream and downstream regions to the *nanB* gene added via isothermal assembly. Strain P2406 was transformed with the PCR product, and the transformants were selected on TSA-kanamycin ($125 \mu\text{g}/\text{ml}$) plates. The *nanA nanB* double-mutant strain (P2545) was constructed by transforming P2511 with genomic DNA from strain P2508, and transformants selected on TSA-chloramphenicol plates.

S. pneumoniae strains were grown statically in tryptic soy broth (TSB [(BD, NJ)] at 37°C to an optical density at 620 nm (OD_{620}) of 1.0. For quantitation, serial dilutions (1:10) of the inoculum or URT lavages were plated on TSA-antibiotic selection plates with $100 \mu\text{l}$ catalase ($30,000 \text{ U}/\text{ml}$; Worthington Biochemical) and incubated overnight (37°C , 5% CO_2). Bacteria were stored in 20% glycerol at -80°C . Colonization of pups was carried out by i.n. instillation of 10^3 CFU in $3 \mu\text{l}$ of PBS 1 or 3 days prior to IAV infection.

qRT-PCR. Following a retrograde URT lavage with $300 \mu\text{l}$ RLT lysis buffer, RNA was isolated (RNeasy kit; Qiagen), and cDNA was generated (high-capacity RT kit; Applied Biosystems) and used for quantitative PCR (SYBR Green PCR master mix; Applied Biosystems). Results were analyzed using the threshold cycle ($2^{-\Delta\Delta\text{CT}}$) method (80) by comparison to GAPDH (glyceraldehyde-3-phosphate dehydrogenase) transcription. Values represent the fold change over uninfected.

ELISA. Immulon 4 HBX plates (Thermo Scientific) were coated with $5 \mu\text{g}/\text{ml}$ purified A/X-31 in coating buffer ($0.015 \text{ M Na}_2\text{CO}_3$ plus 0.035 M NaHCO_3 at $50 \mu\text{l}/\text{well}$) and incubated overnight at 4°C . After three washes with PBS-T (PBS plus 0.1% Tween 20 at $100 \mu\text{l}/\text{well}$), plates were incubated with blocking solution (BS) (PBS-T plus 0.5% milk powder plus 3% goat serum [Thermo Fisher] for 1 h at 20°C). BS was discarded, and mouse sera were diluted to a starting concentration of 1:100 and then serially diluted 1:2 in BS ($100 \mu\text{l}/\text{well}$) and incubated (2 h at 20°C). Three washes with PBS-T were done prior to addition of secondary antibody (horseradish peroxidase [HRP]-labeled anti-mouse IgG [whole antibody] from GE Healthcare or alkaline phosphatase [AP]-labeled anti-mouse IgA [α chain] from Sigma) diluted in BS (1:3,000 at $50 \mu\text{l}/\text{well}$). After incubation (1 h at 20°C) and three washes with PBS-T, plates were developed for 10 min using $100 \mu\text{l}/\text{well}$ SigmaFast OPD (*o*-phenylenediamine dihydrochloride [Sigma]) and stopped with 3 M HCl ($50 \mu\text{l}/\text{well}$) or developed for 1 to 18 h using pNPP (*p*-nitrophenyl phosphate [KPL]). Plates were read at OD_{490} for the OPD substrate or OD_{405} for the AP substrate. The endpoint titers were determined by calculating the dilution at which the absorbance is equal to 0.1. The geometric mean titers (GMTs) were calculated from the reciprocal of the endpoint titers.

Statistical analysis. GraphPad Prism 7 software was used for all statistical analyses. Unless otherwise noted, data were analyzed using the Mann-Whitney *U* test to compare two groups, and the Kruskal-Wallis test with Dunn's postanalysis for multiple group comparisons.

Data availability. The authors confirm that data will be made publicly available upon publication upon request, without restriction. A/X-31 (H3N2) virus was provided by Jan Erickson (University of Pennsylvania).

SUPPLEMENTAL MATERIAL

Supplemental material for this article may be found at <https://doi.org/10.1128/mBio.02359-18>.

FIG S1, EPS file, 0.5 MB.

FIG S2, EPS file, 1.3 MB.

FIG S3, EPS file, 0.8 MB.

FIG S4, EPS file, 1 MB.

FIG S5, EPS file, 0.6 MB.

ACKNOWLEDGMENTS

We thank Elodie Ghedin (NYU) for the sequencing of A/X-31.

M.B.O. was supported by the NYU Division of Infectious Diseases, Department of Medicine Silverman Scholarship, and Physician Scientist Training Program Award; S.B. was supported by the NYU School of Medicine and National Institute of Diabetes & Digestive & Kidney Diseases fellowship. This project was supported by grants from the U.S. Public Health Service to J.N.W. (AI038446 and AI105168).

REFERENCES

- Rolfes MAFI, Garg S, Flannery B, Brammer L, Singleton JA, et al. 2016. Estimated influenza illnesses, medical visits, hospitalizations, and deaths averted by vaccination in the United States. <https://www.cdc.gov/flu/about/disease/2015-16.htm>. Accessed September 2018.
- CDC. 2018. National Press Conference kicks off 2018–2019 flu vaccination campaign. <https://www.cdc.gov/flu/spotlights/press-conference-2018-19.htm#ref1>. Accessed September 2018.
- Flannery B, Reynolds SB, Blanton L, Santibanez TA, O'Halloran A, Lu PJ, Chen J, Foppa IM, Gargiullo P, Bresee J, Singleton JA, Fry AM. 2017. Influenza vaccine effectiveness against pediatric deaths: 2010–2014. *Pediatrics* 139:e20164244. <https://doi.org/10.1542/peds2016-4244>.
- Arriola C, Garg S, Anderson EJ, Ryan PA, George A, Zansky SM, Bennett N, Reingold A, Bargsten M, Miller L, Yousey-Hindes K, Tatham L, Bohm SR, Lynfield R, Thomas A, Lindegren ML, Schaffner W, Fry AM, Chaves SS. 2017. Influenza vaccination modifies disease severity among community-dwelling adults hospitalized with influenza. *Clin Infect Dis* 65:1289–1297. <https://doi.org/10.1093/cid/cix468>.
- CDC. 2014. Selected publications on influenza vaccine effectiveness. <https://www.cdc.gov/flu/about/qa/publications.htm>. Accessed September 2018.
- Lowen AC, Steel J, Mubareka S, Carnero E, Garcia-Sastre A, Palese P. 2009. Blocking interhost transmission of influenza virus by vaccination in the guinea pig model. *J Virol* 83:2803–2818. <https://doi.org/10.1128/JVI.02424-08>.
- Houser KV, Pearce MB, Katz JM, Tumpey TM. 2013. Impact of prior seasonal H3N2 influenza vaccination or infection on protection and transmission of emerging variants of influenza A(H3N2)v virus in ferrets. *J Virol* 87:13480–13489. <https://doi.org/10.1128/JVI.02434-13>.
- CDC. 2018. 2017–18 flu season. <https://www.cdc.gov/flu/fluavxview/1718season.htm>. Accessed October 2018.
- CDC. 2018. Seasonal influenza vaccine effectiveness, 2004–2018. <https://www.cdc.gov/flu/professionals/vaccination/effectiveness-studies.htm>. Accessed October 2018.
- Cheung DH, Tsang TK, Fang VJ, Xu J, Chan KH, Ip DK, Peiris JS, Leung GM, Cowling BJ. 2015. Association of oseltamivir treatment with virus shedding, illness, and household transmission of influenza viruses. *J Infect Dis* 212:391–396. <https://doi.org/10.1093/infdis/jiv058>.
- Ng S, Cowling BJ, Fang VJ, Chan KH, Ip DK, Cheng CK, Uyeki TM, Houck PM, Malik Peiris JS, Leung GM. 2010. Effects of oseltamivir treatment on duration of clinical illness and viral shedding and household transmission of influenza virus. *Clin Infect Dis* 50:707–714. <https://doi.org/10.1086/650458>.
- Hayden FG, Belshe R, Villanueva C, Lanno R, Hughes C, Small I, Dutkowsky R, Ward P, Carr J. 2004. Management of influenza in households: a prospective, randomized comparison of oseltamivir treatment with or without postexposure prophylaxis. *J Infect Dis* 189:440–449. <https://doi.org/10.1086/381128>.
- Welliver R, Monto AS, Carewicz O, Schatteman E, Hassman M, Hedrick J, Jackson HC, Huson L, Ward P, Oxford JS, Oseltamivir Post Exposure Prophylaxis Investigator Group. 2001. Effectiveness of oseltamivir in preventing influenza in household contacts: a randomized controlled trial. *JAMA* 285:748–754. <https://doi.org/10.1001/jama.285.6.748>.
- Halloran ME, Hayden FG, Yang Y, Longini IM, Jr, Monto AS. 2006. Antiviral effects on influenza viral transmission and pathogenicity: observations from household-based trials. *Am J Epidemiol* 165:212–221. <https://doi.org/10.1093/aje/kwj362>.
- Hayward A. 2010. Does treatment with oseltamivir prevent transmission of influenza to household contacts? *Clin Infect Dis* 50:715–716. <https://doi.org/10.1086/650459>.
- Herfst S, Schrauwen EJ, Linster M, Chutinimitkul S, de Wit E, Munster VJ, Sorrell EM, Bestebroer TM, Burke DF, Smith DJ, Rimmelzwaan GF, Osterhaus AD, Fouchier RA. 2012. Airborne transmission of influenza A/H5N1 virus between ferrets. *Science* 336:1534–1541. <https://doi.org/10.1126/science.1213362>.
- Imai M, Watanabe T, Hatta M, Das SC, Ozawa M, Shinya K, Zhong G, Hanson A, Katsura H, Watanabe S, Li C, Kawakami E, Yamada S, Kiso M, Suzuki Y, Maher EA, Neumann G, Kawaoka Y. 2012. Experimental adaptation of an influenza H5 HA confers respiratory droplet transmission to a reassortant H5 HA/H1N1 virus in ferrets. *Nature* 486:420–428. <https://doi.org/10.1038/nature10831>.
- Schrauwen EJ, Fouchier RA. 2014. Host adaptation and transmission of influenza A viruses in mammals. *Emerg Microbes Infect* 3:e9. <https://doi.org/10.1038/emi.2014.9>.
- Lowen AC, Mubareka S, Steel J, Palese P. 2007. Influenza virus transmission is dependent on relative humidity and temperature. *PLoS Pathog* 3:1470–1476. <https://doi.org/10.1371/journal.ppat.0030151>.
- Eaton MD. 1940. Transmission of epidemic influenza virus in mice by contact. *J Bacteriol* 39:229–241.
- Schulman JL, Kilbourne ED. 1962. Airborne transmission of influenza virus infection in mice. *Nature* 195:1129–1130. <https://doi.org/10.1038/1951129a0>.
- Lowen AC, Mubareka S, Tumpey TM, Garcia-Sastre A, Palese P. 2006. The guinea pig as a transmission model for human influenza viruses. *Proc Natl Acad Sci U S A* 103:9988–9992. <https://doi.org/10.1073/pnas.0604157103>.
- Edenborough KM, Gilbertson BP, Brown LE. 2012. A mouse model for the study of contact-dependent transmission of influenza A virus and the factors that govern transmissibility. *J Virol* 86:12544–12551. <https://doi.org/10.1128/JVI.00859-12>.
- Klinkhammer J, Schnepf D, Ye L, Schwaderlapp M, Gad HH, Hartmann R, Garcin D, Mahlakoiv T, Staeheli P. 2018. IFN-lambda prevents influenza virus spread from the upper airways to the lungs and limits virus transmission. *eLife* 7:e33354. <https://doi.org/10.7554/eLife.33354>.
- Diavatopoulos DA, Short KR, Price JT, Wilksch JJ, Brown LE, Briles DE, Strugnell RA, Wijburg OL. 2010. Influenza A virus facilitates *Streptococcus pneumoniae* transmission and disease. *FASEB J* 24:1789–1798. <https://doi.org/10.1096/fj.09-146779>.
- Price GE, Lo CY, Mispion JA, Epstein SL. 2014. Mucosal immunization with a candidate universal influenza vaccine reduces virus transmission in a mouse model. *J Virol* 88:6019–6030. <https://doi.org/10.1128/JVI.03101-13>.
- Wu R, Sui Z, Liu Z, Liang W, Yang K, Xiong Z, Xu D. 2010. Transmission of avian H9N2 influenza viruses in a murine model. *Vet Microbiol* 142:211–216. <https://doi.org/10.1016/j.vetmic.2009.09.068>.
- Rigoni M, Toffan A, Viale E, Mancin M, Cilloni F, Bertoli E, Salomoni A, Marciano S, Milani A, Zecchin B, Capua I, Cattoli G. 2010. The mouse model is suitable for the study of viral factors governing transmission and pathogenesis of highly pathogenic avian influenza (HPAI) viruses in mammals. *Vet Res* 41:66. <https://doi.org/10.1051/vetres/2010038>.
- Ivinson K, Deliyannis G, McNabb L, Grollo L, Gilbertson B, Jackson D, Brown LE. 2017. Salivary blockade protects the lower respiratory tract of

- mice from lethal influenza virus infection. *J Virol* 91:e00624-17. <https://doi.org/10.1128/JVI.00624-17>.
30. Bouvier NM, Lowen AC. 2010. Animal models for influenza virus pathogenesis and transmission. *Viruses* 2:1530–1563. <https://doi.org/10.3390/v20801530>.
 31. Carrat F, Vergu E, Ferguson NM, Lemaître M, Cauchemez S, Leach S, Valleron AJ. 2008. Time lines of infection and disease in human influenza: a review of volunteer challenge studies. *Am J Epidemiol* 167:775–785. <https://doi.org/10.1093/aje/kwm375>.
 32. Schulman JL. 1967. Experimental transmission of influenza virus infection in mice. IV. Relationship of transmissibility of different strains of virus and recovery of airborne virus in the environment of infector mice. *J Exp Med* 125:479–488. <https://doi.org/10.1084/jem.125.3.479>.
 33. Ichinohe T, Pang IK, Kumamoto Y, Peaper DR, Ho JH, Murray TS, Iwasaki A. 2011. Microbiota regulates immune defense against respiratory tract influenza A virus infection. *Proc Natl Acad Sci U S A* 108:5354–5359. <https://doi.org/10.1073/pnas.1019378108>.
 34. Rosshart SP, Vassallo BG, Angeletti D, Hutchinson DS, Morgan AP, Takeda K, Hickman HD, McCulloch JA, Badger JH, Ajami NJ, Trinchieri G, Pardo-Manuel de Villena F, Yewdell JW, Rehermann B. 2017. Wild mouse gut microbiota promotes host fitness and improves disease resistance. *Cell* 171:1015–1028.e13. <https://doi.org/10.1016/j.cell.2017.09.016>.
 35. Lee KH, Gordon A, Shedden K, Kuan G, Ng S, Balmaseda A, Foxman B. 2018. The respiratory microbiome and susceptibility to influenza virus infection. *bioRxiv* <https://doi.org/10.1101/372649>.
 36. Bogaert D, van Belkum A, Sluiter M, Luijendijk A, de Groot R, Rumke HC, Verbrugh HA, Hermans PW. 2004. Colonisation by *Streptococcus pneumoniae* and *Staphylococcus aureus* in healthy children. *Lancet* 363:1871–1872. [https://doi.org/10.1016/S0140-6736\(04\)16357-5](https://doi.org/10.1016/S0140-6736(04)16357-5).
 37. Adler H, Ferreira DM, Gordon SB, Rylance J. 2017. Pneumococcal capsular polysaccharide immunity in the elderly. *Clin Vaccine Immunol* 24:e00004-17. <https://doi.org/10.1128/CVI.00004-17>.
 38. Takano M, Ozaki K, Nitahara Y, Higuchi W, Takano T, Nishiyama A, Yamamoto T. 2009. *Streptococcus pneumoniae* and *Haemophilus influenzae* at the initial stage of influenza. *Pediatr Int* 51:687–695. <https://doi.org/10.1111/j.1442-200X.2009.02861.x>.
 39. Short KR, Habets MN, Hermans PW, Diavatopoulos DA. 2012. Interactions between *Streptococcus pneumoniae* and influenza virus: a mutually beneficial relationship? *Future Microbiol* 7:609–624. <https://doi.org/10.2217/fmb.12.29>.
 40. Zafar MA, Kono M, Wang Y, Zangari T, Weiser JN. 2016. Infant mouse model for the study of shedding and transmission during *Streptococcus pneumoniae* mono-infection. *Infect Immun* 84:2714–2722. <https://doi.org/10.1128/IAI.00416-16>.
 41. Siegel SJ, Roche AM, Weiser JN. 2014. Influenza promotes pneumococcal growth during coinfection by providing host sialylated substrates as a nutrient source. *Cell Host Microbe* 16:55–67. <https://doi.org/10.1016/j.chom.2014.06.005>.
 42. Xu G, Kiefel MJ, Wilson JC, Andrew PW, Oggioni MR, Taylor GL. 2011. Three *Streptococcus pneumoniae* sialidases: three different products. *J Am Chem Soc* 133:1718–1721. <https://doi.org/10.1021/ja110733q>.
 43. Moustafa I, Connaris H, Taylor M, Zaitsev V, Wilson JC, Kiefel MJ, von Itzstein M, Taylor G. 2004. Sialic acid recognition by *Vibrio cholerae* neuraminidase. *J Biol Chem* 279:40819–40826. <https://doi.org/10.1074/jbc.M404965200>.
 44. Yan J, Grantham M, Pantelic J, Bueno de Mesquita PJ, Albert B, Liu F, Ehrman S, Milton DK, EMIT Consortium. 2018. Infectious virus in exhaled breath of symptomatic seasonal influenza cases from a college community. *Proc Natl Acad Sci U S A* 115:1081–1086. <https://doi.org/10.1073/pnas.1716561115>.
 45. Ng S, Lopez R, Kuan G, Gresh L, Balmaseda A, Harris E, Gordon A. 2016. The timeline of influenza virus shedding in children and adults in a household transmission study of influenza in Managua, Nicaragua. *Pediatr Infect Dis J* 35:583–586. <https://doi.org/10.1097/INF.0000000000001083>.
 46. Schulman JL, Kilbourne ED. 1963. Experimental transmission of influenza virus infection in mice. I. The period of transmissibility. *J Exp Med* 118:257–266. <https://doi.org/10.1084/jem.118.2.257>.
 47. Schulman JL, Kilbourne ED. 1963. Experimental transmission of influenza virus infection in mice. II. Some factors affecting the incidence of transmitted infection. *J Exp Med* 118:267–275. <https://doi.org/10.1084/jem.118.2.267>.
 48. Short KR, Reading PC, Wang N, Diavatopoulos DA, Wijburg OL. 2012. Increased nasopharyngeal bacterial titers and local inflammation facilitate transmission of *Streptococcus pneumoniae*. *mBio* 3:e00255-12. <https://doi.org/10.1128/mBio.00255-12>.
 49. Puck JM, Glezen WP, Frank AL, Six HR. 1980. Protection of infants from infection with influenza A virus by transplacentally acquired antibody. *J Infect Dis* 142:844–849. <https://doi.org/10.1093/infdis/142.6.844>.
 50. Reuman PD, Ayoub EM, Small PA. 1987. Effect of passive maternal antibody on influenza illness in children: a prospective study of influenza A in mother-infant pairs. *Pediatr Infect Dis J* 6:398–403. <https://doi.org/10.1097/00006454-198704000-00011>.
 51. Goldman AS. 1993. The immune system of human milk: antimicrobial, anti-inflammatory and immunomodulating properties. *Pediatr Infect Dis J* 12:664–671. <https://doi.org/10.1097/00006454-199308000-00008>.
 52. Slade HB, Schwartz SA. 1987. Mucosal immunity: the immunology of breast milk. *J Allergy Clin Immunol* 80:348–358. [https://doi.org/10.1016/0091-6749\(87\)90041-8](https://doi.org/10.1016/0091-6749(87)90041-8).
 53. Reuman PD, Paganini CM, Ayoub EM, Small PA, Jr. 1983. Maternal-infant transfer of influenza-specific immunity in the mouse. *J Immunol* 130:932–936.
 54. Brambell FW. 1969. The transmission of immune globulins from the mother to the foetal and newborn young. *Proc Nutr Soc* 28:35–41. <https://doi.org/10.1079/PNS19690007>.
 55. Macchiaverni P, Arslanian C, Frazao JB, Palmeira P, Russo M, Verhasselt V, Condino-Neto A. 2011. Mother to child transfer of IgG and IgA antibodies against *Dermatophagoides pteronyssinus*. *Scand J Immunol* 74:619–627. <https://doi.org/10.1111/j.1365-3083.2011.02615.x>.
 56. Palmeira P, Costa-Carvalho BT, Arslanian C, Pontes GN, Nagao AT, Carneiro-Sampaio MM. 2009. Transfer of antibodies across the placenta and in breast milk from mothers on intravenous immunoglobulin. *Pediatr Allergy Immunol* 20:528–535. <https://doi.org/10.1111/j.1399-3038.2008.00828.x>.
 57. Van de Perre P. 2003. Transfer of antibody via mother's milk. *Vaccine* 21:3374–3376. [https://doi.org/10.1016/S0264-410X\(03\)00336-0](https://doi.org/10.1016/S0264-410X(03)00336-0).
 58. Cianga P, Medesan C, Richardson JA, Ghetie V, Ward ES. 1999. Identification and function of neonatal Fc receptor in mammary gland of lactating mice. *Eur J Immunol* 29:2515–2523. [https://doi.org/10.1002/\(SICI\)1521-4141\(199908\)29:08<2515::AID-IMMU2515>3.0.CO;2-D](https://doi.org/10.1002/(SICI)1521-4141(199908)29:08<2515::AID-IMMU2515>3.0.CO;2-D).
 59. Roopenian DC, Akilsh S. 2007. FcRn: the neonatal Fc receptor comes of age. *Nat Rev Immunol* 7:715–725. <https://doi.org/10.1038/nri2155>.
 60. Mackenzie N. 1984. Fc receptor-mediated transport of immunoglobulin across the intestinal epithelium of the neonatal rodent. *Immunol Today* 5:364–366. [https://doi.org/10.1016/0167-5699\(84\)90080-X](https://doi.org/10.1016/0167-5699(84)90080-X).
 61. Israel EJ, Taylor S, Wu Z, Mizoguchi E, Blumberg RS, Bhan A, Simister NE. 1997. Expression of the neonatal Fc receptor, FcRn, on human intestinal epithelial cells. *Immunology* 92:69–74. <https://doi.org/10.1046/j.1365-2567.1997.00326.x>.
 62. Story CM, Mikulska JE, Simister NE. 1994. A major histocompatibility complex class I-like Fc receptor cloned from human placenta: possible role in transfer of immunoglobulin G from mother to fetus. *J Exp Med* 180:2377–2381. <https://doi.org/10.1084/jem.180.6.2377>.
 63. Nunes MC, Cutland CL, Jones S, Hugo A, Madimabe R, Simoes EA, Weinberg A, Madhi SA, Maternal Flu Trial Team. 2016. Duration of infant protection against influenza illness conferred by maternal immunization: secondary analysis of a randomized clinical. *JAMA Pediatr* 170:840–847. <https://doi.org/10.1001/jamapediatrics.2016.0921>.
 64. McCullers JA, Rehg JE. 2002. Lethal synergism between influenza virus and *Streptococcus pneumoniae*: characterization of a mouse model and the role of platelet-activating factor receptor. *J Infect Dis* 186:341–350. <https://doi.org/10.1086/341462>.
 65. Bergelson LD, Bukrinskaya AG, Prokazova NV, Shaposhnikova GI, Kocharov SL, Shevchenko VP, Kornilaeva GV, Fomina-Ageeva EV. 1982. Role of gangliosides in reception of influenza virus. *Eur J Biochem* 128:467–474.
 66. Griffin JA, Basak S, Compans RW. 1983. Effects of hexose starvation and the role of sialic acid in influenza virus release. *Virology* 125:324–334. [https://doi.org/10.1016/0042-6822\(83\)90205-2](https://doi.org/10.1016/0042-6822(83)90205-2).
 67. Air GM, Laver WG. 1995. Red cells bound to influenza virus N9 neuraminidase are not released by the N9 neuraminidase activity. *Virology* 211:278–284. <https://doi.org/10.1006/viro.1995.1401>.
 68. Thompson CI, Barclay WS, Zambon MC, Pickles RJ. 2006. Infection of human airway epithelium by human and avian strains of influenza A virus. *J Virol* 80:8060–8068. <https://doi.org/10.1128/JVI.00384-06>.
 69. Malakhov MP, Aschenbrenner LM, Smee DF, Wandersee MK, Sidwell RW, Gubareva LV, Mishin VP, Hayden FG, Kim DH, Ing A, Campbell ER, Yu M, Fang F. 2006. Sialidase fusion protein as a novel broad-spectrum inhib-

- itor of influenza virus infection. *Antimicrob Agents Chemother* 50: 1470–1479. <https://doi.org/10.1128/AAC.50.4.1470-1479.2006>.
70. Nicholls JM, Moss RB, Haslam SM. 2013. The use of sialidase therapy for respiratory viral infections. *Antiviral Res* 98:401–409. <https://doi.org/10.1016/j.antiviral.2013.04.012>.
 71. Triana-Baltzer GB, Gubareva LV, Nicholls JM, Pearce MB, Mishin VP, Belser JA, Chen LM, Chan RW, Chan MC, Hedlund M, Larson JL, Moss RB, Katz JM, Tumpey TM, Fang F. 2009. Novel pandemic influenza A(H1N1) viruses are potently inhibited by DAS181, a sialidase fusion protein. *PLoS One* 4:e7788. <https://doi.org/10.1371/journal.pone.0007788>.
 72. Salvatore M, Satlin MJ, Jacobs SE, Jenkins SG, Schuetz AN, Moss RB, Van Besien K, Shore T, Soave R. 2016. DAS181 for treatment of parainfluenza virus infections in hematopoietic stem cell transplant recipients at a single center. *Biol Blood Marrow Transplant* 22:965–970. <https://doi.org/10.1016/j.bbmt.2016.02.011>.
 73. National Institutes of Health. 2015. Public Health Service policy on humane care and use of laboratory animals. Office of Laboratory Animal Welfare, National Institutes of Health, Bethesda, MD.
 74. Public Health Service. 2009. Biosafety in microbiological and medical laboratories, 5th ed. Department of Health and Human Services, Public Health Service, National Institutes of Health, Bethesda, MD.
 75. Baer A, Kehn-Hall K. 2014. Viral concentration determination through plaque assays: using traditional and novel overlay systems. *J Vis Exp* 4:e52065. <https://doi.org/10.3791/52065>.
 76. Reed LJ, Muench H. 1938. A simple method of estimating fifty per cent endpoints. *Am J Epidemiol* 27:493–497. <https://doi.org/10.1093/oxfordjournals.aje.a118408>.
 77. Dalia AB, Standish AJ, Weiser JN. 2010. Three surface exoglycosidases from *Streptococcus pneumoniae*, NanA, BgaA, and StrH, promote resistance to opsonophagocytic killing by human neutrophils. *Infect Immun* 78:2108–2116. <https://doi.org/10.1128/IAI.01125-09>.
 78. Sung CK, Li H, Claverys JP, Morrison DA. 2001. An rpsL cassette, Janus, for gene replacement through negative selection in *Streptococcus pneumoniae*. *Appl Environ Microbiol* 67:5190–5196. <https://doi.org/10.1128/AEM.67.11.5190-5196.2001>.
 79. Lemon JK, Weiser JN. 2015. Degradation products of the extracellular pathogen *Streptococcus pneumoniae* access the cytosol via its pore-forming toxin. *mBio* 6:e02110-14. <https://doi.org/10.1128/mBio.02110-14>.
 80. Livak KJ, Schmittgen TD. 2001. Analysis of relative gene expression data using real-time quantitative PCR and the $2^{-\Delta\Delta CT}$ method. *Methods* 25:402–408. <https://doi.org/10.1006/meth.2001.1262>.